

# Integrated System for Point Cloud Reconstruction and Simulated Brain Shift Validation Using Tracked Surgical Microscope

Xiaochen Yang<sup>1</sup>, Logan W. Clements<sup>2</sup>, Ma Luo<sup>2</sup>, Saramati Narasimhan<sup>2</sup>, Reid C. Thompson<sup>3</sup>,  
Benoit M. Dawant<sup>1,2,4</sup>, and Michael I. Miga<sup>2,3,4</sup>

<sup>1</sup>Vanderbilt University, Department of Electrical Engineering and Computer Science,  
Nashville, TN USA

<sup>2</sup>Vanderbilt University, Department of Biomedical Engineering, Nashville, TN USA

<sup>3</sup>Vanderbilt University Medical Center, Department of Neurological Surgery, Nashville, TN  
USA

<sup>4</sup>Vanderbilt University Medical Center, Department of Radiology, Nashville, TN USA

## ABSTRACT

Intra-operative soft tissue deformation, referred to as brain shift, compromises the application of current image-guided surgery (IGS) navigation systems in neurosurgery. A computational model driven by sparse data has been proposed as a cost effective method to compensate for cortical surface and volumetric displacements. Stereoscopic microscopes and laser range scanners (LRS) are the two most investigated sparse intra-operative imaging modalities for driving these systems. However, integrating these devices in the clinical workflow to facilitate development and evaluation requires developing systems that easily permit data acquisition and processing. In this work we present a mock environment developed to acquire stereo images from a tracked operating microscope and to reconstruct 3D point clouds from these images. A reconstruction error of 1 mm is estimated by using a phantom with a known geometry and independently measured deformation extent. The microscope is tracked via an attached tracking rigid body that facilitates the recording of the position of the microscope via a commercial optical tracking system as it moves during the procedure. Point clouds, reconstructed under different microscope positions, are registered into the same space in order to compute the feature displacements. Using our mock craniotomy device, realistic cortical deformations are generated. Our experimental results report approximately 2mm average displacement error compared with the optical tracking system. These results demonstrate the practicality of using tracked stereoscopic microscope as an alternative to LRS to collect sufficient intraoperative information for brain shift correction.

**Keywords:** Brain shift, stereoscopic microscope, intra-operative imaging, stereopsis, reconstruction, tracking, accuracy

## 1. INTRODUCTION

Image-guided surgery (IGS) [1] provides a standard of care platform for guiding surgeons during brain tumor resection. Unfortunately, commercial IGS navigation systems do not have mechanisms to account for non-rigid tissue deformations which commonly arise from cerebrospinal fluid drainage, tissue swelling due to edema, tissue contraction due hyperosmotic drugs, or tissue retraction/resection [2]. Solutions like intraoperative magnetic resonance (iMR) imaging [3], intraoperative computed tomography (iCT) [4], or intraoperative ultrasound (iUS) [5] have been proposed to compensate for soft-tissue changes. However, deficiencies like ionizing radiation of iCT, high cost of iMR, and poor image contrast/quality of iUS have compelled researchers to look for alternatives. Another cost effective method is to use sparse data acquired intraoperatively to update a computer-based model [6]. Laser range scanners (LRS) and stereoscopic microscopes are two widely used surface data acquisition

---

Further author information:

Xiaochen Yang: E-mail: xiaochen.yang@vanderbilt.edu

techniques [7][8]. Both devices can be used in an operating room (OR) and generate three-dimensional cortical surface cloud data as well as a texture map. Typically, the microscope is continuously used during the whole surgery. Thus, it can provide high-resolution, consistent intraoperative information in near real-time with very limited interruption to the surgical workflow. Performing a single LRS acquisition is more disruptive because it takes about 30 seconds and requires the surgical microscope to be moved away from the surgical field of view. In recent work, we demonstrated position-fixed stereo-pair cameras for surface measurements. This work used two identical Grasshopper digital cameras produced by Point Grey Research, Inc. (Richmond, British Columbia, Canada) and served as an initial testing prototype for our mock cortical surface environment [9].

In the work reported here, we have extended those approaches to a surgical microscope that is used clinically at our institution. We have developed an interactive environment that permits acquisition of stereo image capture from the microscope, calibration of the cameras, and adjustment of parameters used for 3D point cloud reconstruction. We have also equipped the microscope with a rigid body tracking star (MICROSCOPE TRACKING ARRAY, Brainlab Inc., Westchester, IL) to permit tracking of the microscope position within an IGS system. We show that with this device we can register 3D point clouds that are acquired with the microscope in different positions thus permitting an intraoperative calculation of cortical surface displacement. While the availability of microscope focal point tracking is possible with commercial IGS systems (although accuracy on these commercial systems is not widely reported), the implementation of a fully 3D tracked approach necessary for measuring full cortical surface field displacements is lacking.

## 2. METHODS

### 2.1 Data acquisition

At Vanderbilt University Medical Center (VUMC) OPMI Pentero (Carl Zeiss, Inc., Oberkochen, Germany) surgical microscopes are routinely used during neurosurgery procedures. The scope used for this study is equipped with two charged-coupled device (CCD) cameras, Zeiss MediLive Trio, with a video frame rate of approximately 30 frames per second (FPS). The images or video stream in the field of view (FOV) can be displayed on touchscreen monitor, controlled using a joystick, recorded, and exported by video output interface. Through an IEEE 1394 interface, captured data can be saved on a desktop or laptop (see Figure 1 left). In our previous work, a user-friendly graphical user interface (GUI) was proposed to facilitate the acquisition and was designed to be compatible with all USB, Point Grey Research or other IEEE-1394b (FireWire) digital cameras [9] [10].



Figure 1. System overview with simulated craniotomy device and calibration phantom

### 2.2 Reconstruction system

Point cloud reconstruction from microscopic stereo-pair images requires several steps: camera calibration, image rectification, disparity computation, and 3D point cloud reconstruction. Each of these steps may require parameter adjustments to produce acceptable results. To facilitate the process and make it achievable by users that are

not experts in computer vision, we have developed an interactive environment. This environment includes a GUI through which parameters can be adjusted using check-boxes, spin-boxes, and line-edit widgets. Intermediate and final results are also shown. This GUI is written in C++ using Qt [11] and can be run on Windows and Linux platforms. We used the OpenCV library [12] for the computer vision algorithms, and the PCL library [13] was used to display and process point cloud data.

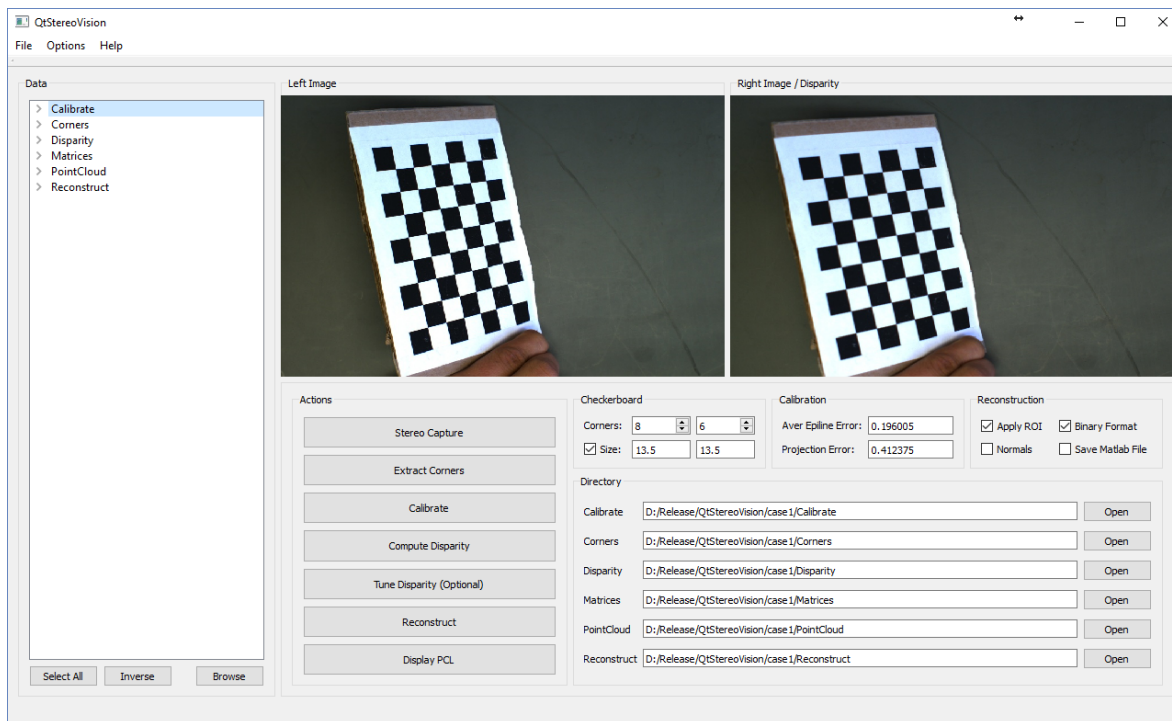


Figure 2. Integrated reconstruction software: main window

Figure 2 shows the main window of the software. On the left side of the interface is a tree-view structure is used to select the input images, the output point clouds, as well as some intermediate results. Moving to the right, a display area facilitates visualization of the stereo-pair images (left and right), and the panel below contains the series of actions and options necessary to perform the point cloud reconstruction. The first step involves stereo capture of a calibration checkerboard pattern and the user is guided through the process. The next step is the localization of the corners in the checkerboard images and the calibration of the stereo cameras using the method described in [14].

Once the calibration is complete, the output camera matrices are used to rectify left and right images. The disparity map can then be computed using either a block matching (BM) or a semi-global block matching (SGBM) algorithm [15]. Both BM and SGBM algorithms use nine parameters that can be adjusted. These can be adjusted using sliders while showing the disparity image produced by the current parameter values (see Figure 3). Once the disparity image computation is deemed acceptable by the user, the point cloud can be computed for each disparity image. After computing the reconstruction [16], the display panel is invoked to immediately provide a visualization of the point clouds.

### 2.3 Microscope tracking

Microscope tracking can be performed via the use of a rigidly attached optically tracked reference body and a calibration procedure to compute the transformation between the coordinate system specified by the rigid tracking body and the coordinate system of the reconstructed stereo-pair point cloud [17]. We use a Polaris Spectra optical tracking system developed by Northern Digital, Inc. (Waterloo, Ontario, Canada) which has a reported tracking accuracy of 0.25-0.3mm RMS [18]. A commercially available rigid body reference with

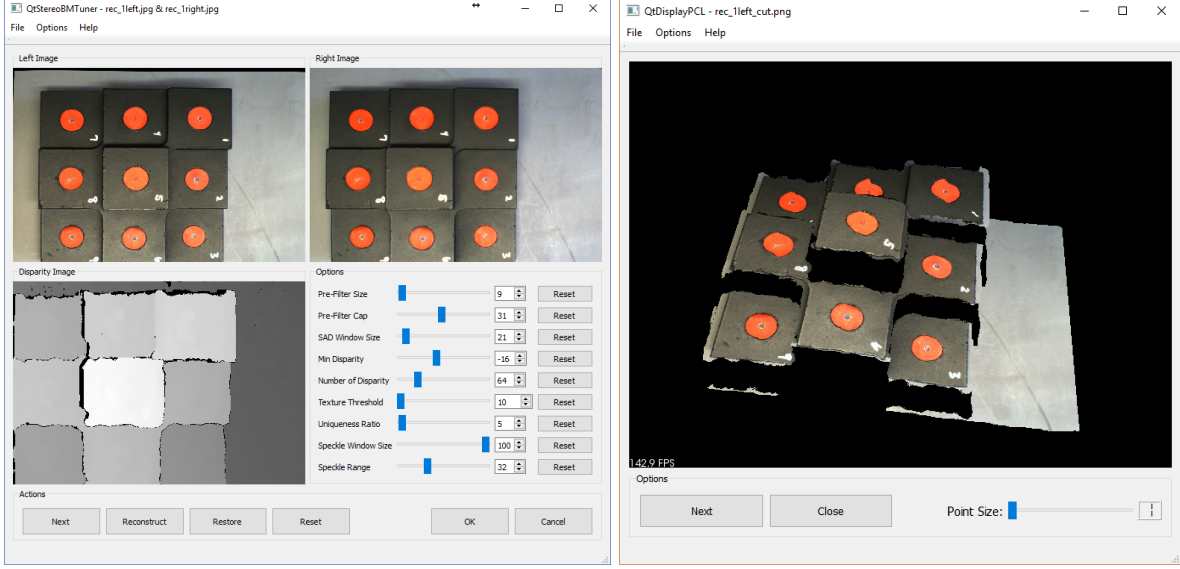


Figure 3. Integrated reconstruction software: disparity tuner panel, and point cloud display window

microscope mounting attachment (MICROSCOPE TRACKING ARRAY, Brainlab Inc., Westchester, IL) was employed to facilitate tracking of the surgical microscope.

The setup for microscope tracking calibration is sketched in Figure 4 (left). To summarize, the goal of the microscope tracking calibration is to determine the rigid body transform that provides a mapping between the coordinate system of the reconstructed stereo-pair point cloud ( $X_{cam}$ ) and the coordinate system of the rigid body attached to the surgical microscope ( $X_{star}$ ). This calibration transform ( $T_{cam-star}$ ) is computed using a calibration phantom that is comprised of a series of fiducial disks that can be localized in both the reconstructed stereo-pair point cloud space and the coordinate system space of the microscope rigid body. The fiducial points are located in the reconstructed stereo-pair space via computation of disk centroids from the reconstructed point cloud. The fiducial point locations in the microscope rigid body space are determined via an optically tracked probe that can digitize the individual fiducial points relative to the microscope rigid body within the optical tracking system. Once these individual fiducial points have been localized in each space, a point-based registration [19] is computed to determine the camera calibration transform ( $T_{cam-star}$ ).

An experiment to validate the microscope tracking calibration transform ( $T_{cam-star}$ ) is shown in Figure 4 (right). At an initial position of the surgical microscope ( $X_{cam,1}$ ), the tracked location of the scanner was recorded ( $T_{star-opt,1}$ ) and a stereo-pair reconstruction was performed of the calibration phantom. With the phantom and optical tracking system in a fixed position, the surgical microscope was then moved to a second position ( $X_{cam,2}$ ). Again, the tracked location of the scanner was recorded ( $T_{star-opt,2}$ ) and a stereo-pair reconstruction was performed. Given the recorded data from the two locations, the fixed microscope calibration transformation ( $T_{cam-star}$ ) and the fixed optical tracking coordinate system ( $X_{opt}$ ), the stereo-pair reconstructed point clouds acquired at the two microscope locations can be transformed into the same space using the following equations:

$$X_{opt} = [T_{star \rightarrow opt,1}] [T_{cam \rightarrow star}] X_{cam,1} \quad (1)$$

$$X_{opt} = [T_{star \rightarrow opt,2}] [T_{cam \rightarrow star}] X_{cam,2} \quad (2)$$

## 2.4 Validation experiment

The validation experiment includes two parts: microscope tracking validation and vessel displacement validation. The aim of the microscope tracking validation is to ensure that the calibration transformation is accurate via

the transformation of a series of point cloud reconstructions, acquired at different microscope locations, to a reference coordinate space. The steps are as follows:

1. Place the scope at base position, then put the calibration phantom under the scope. Reconstruct the point cloud of the phantom.
2. Digitize nine centroid of the disk and record the position of the scope using optical tracking system. The transformation matrix can be computed.
3. Move the scope to another position, while keep the phantom static. Reconstruct the phantom and record the scope position.
4. Repeat step 3.
5. Use the transformation matrix from step 2 to transform the point cloud in step 3 and 4 back to base position and then evaluate the error.

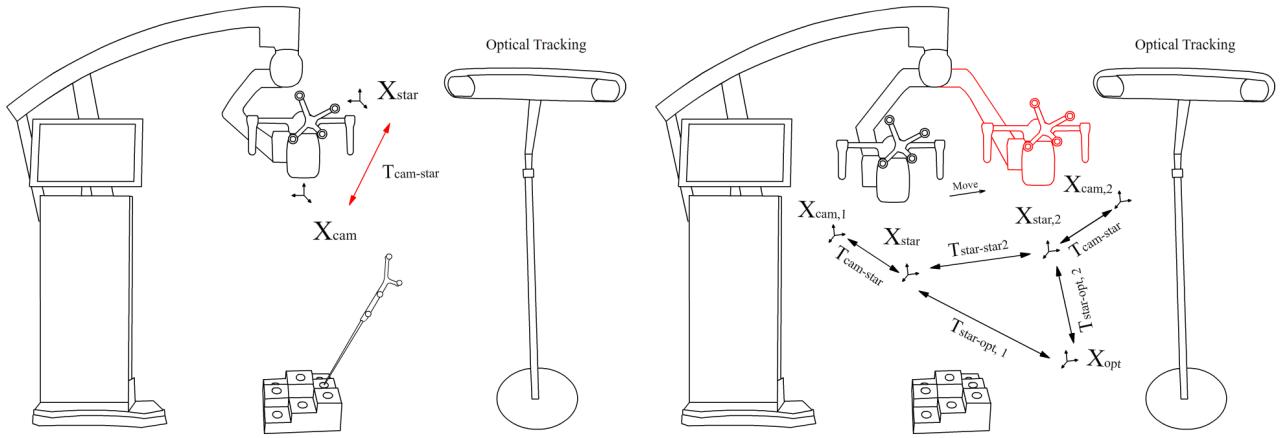


Figure 4. The setup of calibration procedure (left) and tracking experiment (right)

For the vessel displacement computation, we use the craniotomy device to simulate brain shift via three states (baseline, stretch, and sag in Figure 5). The experimental steps are as follows:

1. Set the craniotomy device in the baseline state and place it under the scope.
2. Reconstruct the 3D point cloud of the device and record the ground truth positions of vessel features marked on the membrane using optical tracking system.
3. Move the scope to a new position, and apply a 2 cm horizontal stretch (lateral shift) using the screw mechanism. Then repeat step 2.
4. Move the scope to another new position, and using the four screws around the craniotomy to displace downward by 1.6 cm (similar to sag). Then repeat step 2.
5. Using the previous transformation matrix to transform point cloud in step 3 and step 4 to base space. The movement of features marked on the membrane can be computed after the application of the tracking transformations.

As validation, the deformations are recorded using the optically tracked stylus, which serves as the ground truth and which can be subsequently compared to the tracked microscope stereo pair measurements.

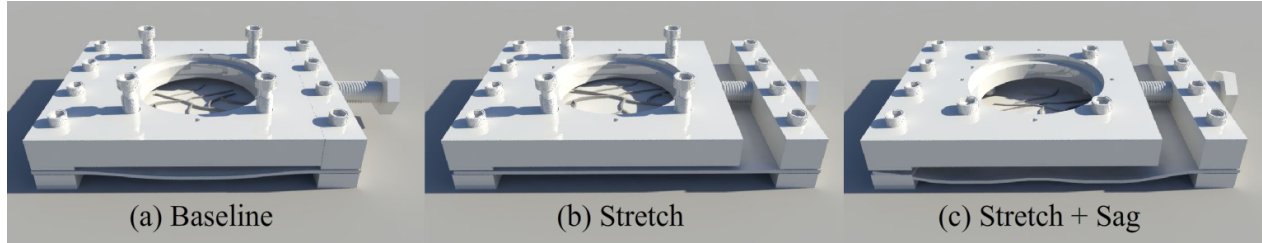


Figure 5. Three states of generating simulated brain shift: baseline, stretch (lateral shift), stretch as well as sag

### 3. RESULTS

The result of the stereo-pair camera calibration for the validation experiment is shown in the GUI. The average epilene error is 0.2 pixels, and the stereo projection error is reported as 0.41 pixels. Knowing the geometry of the calibration phantom, the reconstruction error of approximately 1 mm is estimated by systematically comparing the distance between nine divots. Since the microscope is tracked, the transformation between point clouds generated via scope acquisitions at different positions can be computed. We reconstructed the point cloud of the calibration phantom by moving the scope to three positions (see Figure 6 (a) (b) (c)).

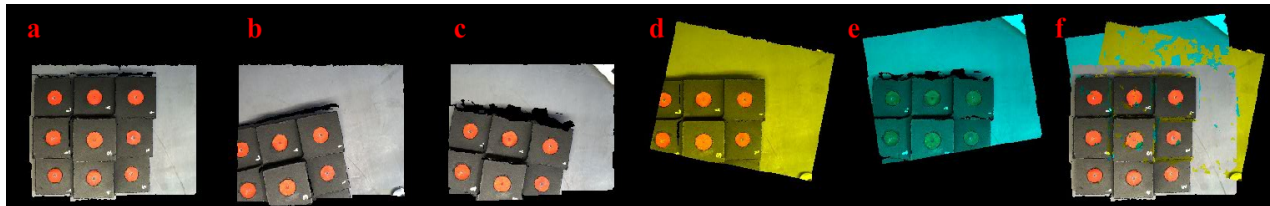


Figure 6. Register point cloud reconstructed from different microscope position to same space

By applying the transformation matrix on the second and third point clouds (highlighted in yellow and blue, respectively, in Figure 6), these two point clouds can be transformed into the same space as the initial point cloud (see Figure 6 (d) (e)). Figure 6 (f) shows the results of registering all three point clouds together. The mean distance error is 0.64 mm in x axis, 0.89 mm in y axis, and 2.92 mm in z axis, which is caused by reconstruction error and tracking error. The displacement is computed by registering the simulated vessel features on simulated craniotomy device to the same space (baseline state) shown in Figure 7. Note that feature No.1 is missing during the stretch (lateral shift) operation of the craniotomy device which also possibly happened in real surgery. The difference between displacement in stereopsis (measured in 3D point cloud) and tracking system (ground truth) is calculated as displacement error which is approximately 2 mm on average (see Figure 8).

### 4. DISCUSSIONS

The phantom experiments performed for the purposes of validating the tracking calibration for the surgical microscope yield a number of error metrics that provide some insight into the range of possible error sources that are contributing factors. These contributing factors include the error due to the stereo-pair reconstruction process, manual error associated with the fiducial digitization and centroid extraction, sub-optimal calibration phantom design and the tracking error associated with the rigid body attachment to the microscope and the tracked stylus.

The stereo-pair reconstruction error highly depends on the quality of disparity computation. Camera calibration decides the result of rectification, which is the crucial step of computing disparity. The scope tracking error is computed by comparing the point clouds that are transformed to the same scope coordinates. The X, Y, and Z axis mean distance errors are computed respectively. The error of Z axis direction is higher than the other two directions which may due to the error of estimating depth from disparity computation. The point cloud reconstruction is more accurate in horizontal direction than in vertical direction. Considering the maximum height

difference of the stairs on the phantom is nearly 50mm (larger than the normal reported brain deformation), the mean distance error is somehow acceptable. Since the stereo reconstruction techniques is not doing well on the sharp edges on stair phantom, one possible way to improve the result is to use different phantom that have no sharp edges, for example, a sphere phantom.

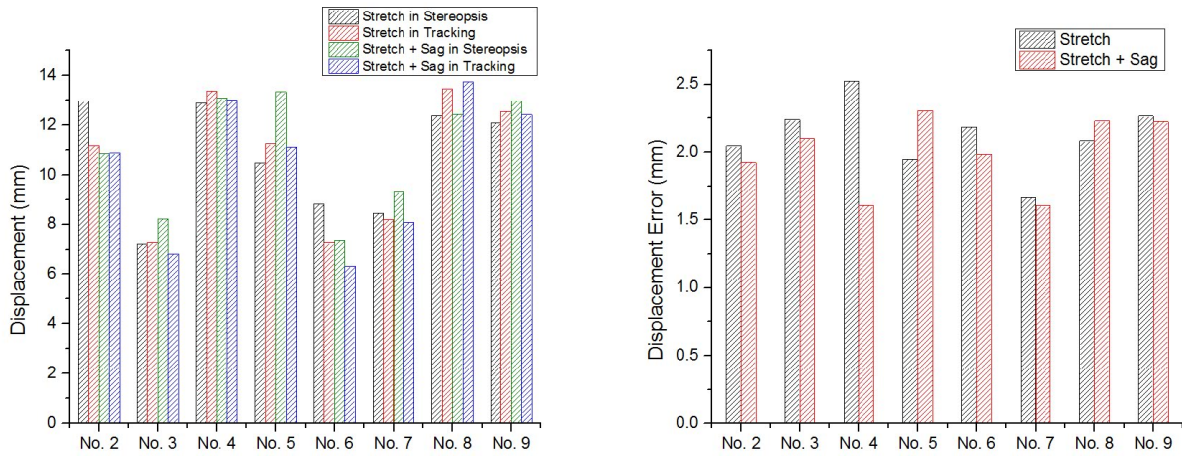


Figure 7. Line of displacement and displacement error

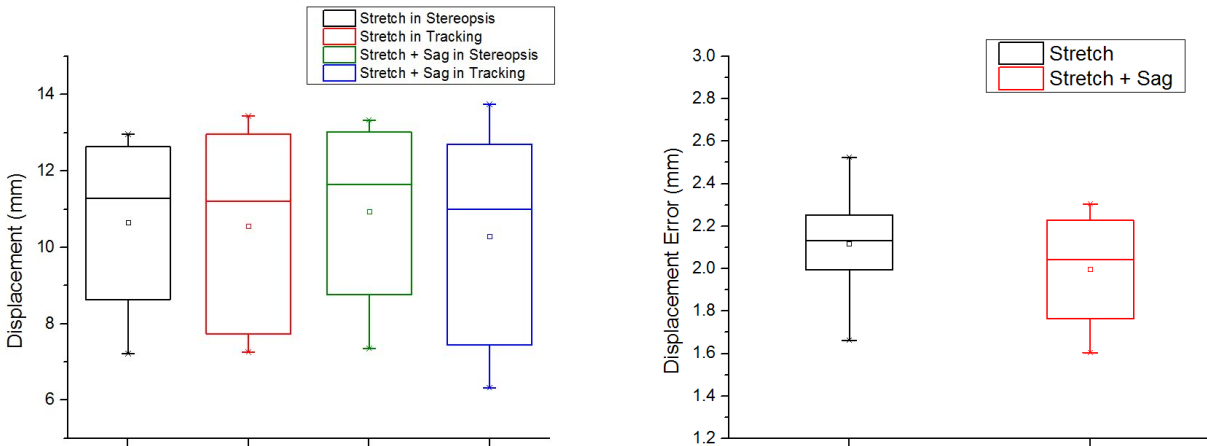


Figure 8. Box plot of displacement and displacement error

Moreover, the error of the tracking system itself and the localization error of using tracking stylus also contribute to the calibration error of the surgical microscope. Error associated with the tracking system used in these experiments is reported by the manufacturer and within an acceptable range. However, any errors associated with the calibration files generated for the tracking of the rigid body attached to the microscope as well as the tracked probe can be potential sources of error. Finally, any manual errors in the digitization of the points on the calibration phantom with the optically tracked probe can introduce errors.

The main goal of this work is to demonstrate the ability to take advantage of stereovision based techniques to track the tissue deformations with arbitrary movement of the surgical microscope. While the results presented indicate that the presented method of microscope tracking calibration is promising, there are a number of avenues for improving the calibration results. Primarily, refinement in reconstruction techniques should facilitate more accurate calibrations when the fidelity of the reconstruction of the calibration phantom is improved. Additionally,

the use of an optimally designed calibration phantom should facilitate more accurate results. Finally, our calibration method is only useful for fixed microscope setting where the focal length and zoom factor cannot change during the whole procedure. Future methods will entail the ability to generate calibration data that allows the use of multiple microscope settings throughout the surgical procedure.

## 5. CONCLUSIONS

In this paper, we have proposed a GUI-based system that integrates all necessary functionality for reconstructing FOV of stereo-pair or microscope cameras including (1) capturing stereo-pair images or video streams, (2) extracting checkerboard corners, (3) calibrating stereo cameras, (4) computing disparity, and (5) displaying point clouds. Moreover, the parameters associated with the disparity computation can be modified in a visualized GUI to improve the results. This reconstruction system is functional and user-friendly. It can be used by people with minimal prior knowledge. By applying image-to-physical space registration, the stereoscopic microscope can be tracked, and freely moved without disrupting the surgical procedure. The reconstruction accuracy and comparison results demonstrate that this system can gather valid cortical data to measure and compensate for brain shift during image-guided surgery, which extends the capability of conventional navigation system.

## ACKNOWLEDGMENTS

This work is funded by the National Institutes of Health, National Institute for Neurological Disorders and Stroke grant number R01-NS049251. We would like to acknowledge Zeiss, Inc., Point Grey Research, Inc., and Northern Digital, Inc. for providing essential equipment and resources, and John Fellenstein from the Vanderbilt Machine Shop for his assistance in our cortical surface deformation simulation device. We would also like to acknowledge Joselito Tiamson, Kim Robertson, and Carol Talbot for their assistance in using Pentero research microscope in an operating room of Vanderbilt University Medical Center (VUMC) to apply our experiments.

## REFERENCES

- [1] Galloway Jr, R. L., “The process and development of image-guided procedures,” *Annual Review of Biomedical Engineering* **3**(1), 83–108 (2001).
- [2] Nabavi, A., Black, P. M., Gering, D. T., Westin, C.-F., Mehta, V., Pergolizzi Jr, R. S., Ferrant, M., Warfield, S. K., Hata, N., Schwartz, R. B., et al., “Serial intraoperative magnetic resonance imaging of brain shift,” *Neurosurgery* **48**(4), 787–798 (2001).
- [3] Nimsy, C., Ganslandt, O., Cerny, S., Hastreiter, P., Greiner, G., and Fahlbusch, R., “Quantification of, visualization of, and compensation for brain shift using intraoperative magnetic resonance imaging,” *Neurosurgery* **47**(5), 1070–1080 (2000).
- [4] Gunnarsson, T., Theodorsson, A., Karlsson, P., Fridriksson, S., Boström, S., Persliden, J., Johansson, I., and Hillman, J., “Mobile computerized tomography scanning in the neurosurgery intensive care unit: increase in patient safety and reduction of staff workload,” *Journal of neurosurgery* **93**(3), 432–436 (2000).
- [5] Unsgaard, G., Rygh, O., Selbekk, T., Müller, T., Kolstad, F., Lindseth, F., and Hernes, T. N., “Intraoperative 3d ultrasound in neurosurgery,” *Acta neurochirurgica* **148**(3), 235–253 (2006).
- [6] Miga, M. I., Roberts, D. W., Kennedy, F. E., Platenik, L. A., Hartov, A., Lunn, K. E., and Paulsen, K. D., “Modeling of retraction and resection for intraoperative updating of images,” *Neurosurgery* **49**(1), 75–85 (2001).
- [7] Miga, M. I., Sinha, T. K., Cash, D. M., Galloway, R. L., and Weil, R. J., “Cortical surface registration for image-guided neurosurgery using laser-range scanning,” *IEEE Transactions on medical Imaging* **22**(8), 973–985 (2003).
- [8] Kumar, A. N., Miga, M. I., Pheiffer, T. S., Chambless, L. B., Thompson, R. C., and Dawant, B. M., “Persistent and automatic intraoperative 3d digitization of surfaces under dynamic magnifications of an operating microscope,” *Medical image analysis* **19**(1), 30–45 (2015).
- [9] Yang, X., Clements, L. W., Conley, R. H., Thompson, R. C., Dawant, B. M., and Miga, M. I., “A novel craniotomy simulation system for evaluation of stereo-pair reconstruction fidelity and tracking,” in [*SPIE Medical Imaging*], 978612–978612, International Society for Optics and Photonics (2016).

- [10] Yang, X., “Stereo-pair Capture Software.” Vanderbilt.edu <https://my.vanderbilt.edu/xiaochen/archives/75>. (Accessed: August 2015).
- [11] “Qt Powerful, Interactive and Corss-Platform Applications.” <https://www.qt.io/>. (Accessed: July 2016).
- [12] Bradski, G. and Kaehler, A., [*Learning OpenCV: Computer vision with the OpenCV library*], ” O’Reilly Media, Inc.” (2008).
- [13] “Point Cloud Library.” <https://www.qt.io/>. (Accessed: July 2016).
- [14] Zhang, Z., “A flexible new technique for camera calibration,” *IEEE Transactions on pattern analysis and machine intelligence* **22**(11), 1330–1334 (2000).
- [15] Scharstein, D. and Szeliski, R., “A taxonomy and evaluation of dense two-frame stereo correspondence algorithms,” *International journal of computer vision* **47**(1-3), 7–42 (2002).
- [16] Hartley, R. and Zisserman, A., [*Multiple view geometry in computer vision*], Cambridge university press (2003).
- [17] Cash, D. M., Sinha, T. K., Chapman, W. C., Terawaki, H., Dawant, B. M., Galloway, R. L., and Miga, M. I., “Incorporation of a laser range scanner into image-guided liver surgery: Surface acquisition, registration, and tracking,” *Medical Physics* **30**(7), 1671–1682 (2003).
- [18] Spectra, P., “Polaris Optical Tracking System.” <http://www.ndigital.com/medical/products/polaris-family/>. (Accessed: July 2016).
- [19] Fitzpatrick, M., “Algorithms for Registration, Error Prediction, and Rotation Parameter Conversion in Matlab.” [http://eecs.vanderbilt.edu/people/mikefitzpatrick/computer%20programs/computer\\_algorithms\\_in\\_Matlab.htm](http://eecs.vanderbilt.edu/people/mikefitzpatrick/computer%20programs/computer_algorithms_in_Matlab.htm). (Accessed: July 2016).